Original Article
ISSN (Online): 2582-7472

ShodhKosh: Journal of Visual and Performing Arts
July-December 2021 2(2), 443–451

STUDY OF STEADY STATE THERMAL STRESSES IN A LIMITING THICK CIRCULAR PLATE WITH INTERNAL HEAT GENERATION

Chetana Bhongade [2]

[1] Department of Mathematics, Shree Shivaji Arts, Commerce & Science College, Rajura, pin:442905, Maharashtra, India

Corresponding Author

Chetana Bhongade,
bhongade.chetana@gmail.com

DOI
10.29121/shodhkosh.v2.i2.2021.5682

Funding: This research received no specific grant from any funding agency in the public, commercial, or not-for-profit sectors.

ABSTRACT

The present paper deals with the determination of temperature, displacement and thermal stresses in a limiting thick circular plate with internal heat generation. A limiting thick circular plate is subjected to arbitrary known interior temperature under steady state, the fixed circular edge of limiting circular plate are thermally insulated and lower surface of limiting circular plate is kept at zero temperature. Here we compute the effects of internal heat generation in terms of stresses along radial direction and modify Kulkarni V. S. (2008). The governing heat conduction equation has been solved by the method of integral transform technique. The results are obtained in a series form in terms of Bessel's functions. The results for stresses have been computed numerically and illustrated graphically.

Keywords: Thermal Stresses, Limiting Thick Circular Plate and Internal Heat Generation

1. INTRODUCTION

The thermoelastic problem consists of determination of the temperature of the heating medium, the heat flux on the boundary surfaces of the limiting thick circular plate when the conditions of the displacement and stresses are known at the some points of the limiting thick circular plate under consideration. Noda et al. (1989) discussed an analytical method for an inverse problem of three dimensional transient thermoelasticity in a transversely isotropic solid by integral transform technique with newly designed potential function and illustrated practical applicability of the method in engineering problem. Kulkarni V. S. (2008) studied an inverse quasi static steady state thermal stresses in a thick circular plate. Bhongade and Durge (2013) considered thick circular plate and discuss, effect of Michell function on steady state behavior of thick circular plate, now here we consider a limiting thick circular plate with internal heat generation subjected to arbitrary known interior temperature. Under steady state, the fixed circular edge of limiting thick circular plate is thermally insulated, lower surface of limiting thick circular plate is at zero temperature and limiting thick circular plate is subjected to arbitrary known interior temperature. Here we compute the effects of internal heat generation on the limiting thick circular plate in terms of stresses along radial direction and we modify Kulkarni V. S. (2008). The governing heat conduction equation has been solved by the method of integral transform technique. The results are obtained in a series form in terms of Bessel's functions. A mathematical model has been constructed for limiting thick circular plate with the help of numerical illustration by considering aluminum (pure) circular plate.

FORMULATION OF THE PROBLEM

Consider a limiting thick circular plate of thickness 2h defined by $0 \leq r \leq a, -h \leq z \leq h$. Let the plate be subjected to arbitrary known interior temperature f(r) within region $-h<z<h$. With circular surface r=a is thermally insulated and lower surface z=-h is kept at zero temperature. Assume the boundary of a limiting thick circular plate is free from traction. Under these prescribed conditions, the thermal steady state temperature, displacement and stresses in a limiting thick circular plate with internal heat generation are required to be determined.

The differential equation governing the displacement potential function ϕ(r,z) is given in Noda (2003) as

$$\frac{\partial^2 \phi}{\partial r^2} + \frac{1}{r}\frac{\partial \phi}{\partial r} + \frac{\partial^2 \phi}{\partial z^2} = K\boldsymbol{\tau} \tag{1}$$

where K is the restraint coefficient and temperature change $\tau = T - T_i$, T_i i is ambient temperature. Displacement function ϕ is known as Goodier's thermoelastic displacement potential.

The steady state temperature $T(r,z)$ of the plate satisfying heat conduction equation as follows,

$$\frac{\partial^2 T}{\partial r^2} + \frac{1}{r}\frac{\partial T}{\partial r} + \frac{\partial^2 T}{\partial z^2} + \frac{q}{k} = 0 \tag{2}$$

with the conditions

$$\frac{\partial T}{\partial r} = 0 \ \ at \ \ r = a, \ -h \leq z \leq h \tag{3}$$

$$T = 0 \ \ at \ z = -h, \ 0 \leq r \leq a \tag{4}$$

$$T = f(r) \ (known) \ at \ \ z = \xi \ , \ -h < \xi < h, 0 \leq r \leq a \tag{5}$$

and

$$T = g(r) \ (\text{unknown}) \text{ at } \ z = h \ , \ 0 \leq r \leq a \tag{6}$$

where k is the thermal conductivity of the material of the plate, q is internal heat generation.

The Michell's function M must satisfy

$$\nabla^2\nabla^2 M = 0 \tag{7}$$

where

$$\nabla^2 = \frac{\partial^2}{\partial r^2} + \frac{1}{r}\frac{\partial}{\partial r} + \frac{\partial^2}{\partial z^2}$$

The components of the stresses are represented by the thermoelastic displacement potential ϕ and Michell's function M as

$$\sigma_{rr} = 2G\left\{\frac{\partial^2 \phi}{\partial r^2} - K\tau + \frac{\partial}{\partial z}\left[\nu\nabla^2 M - \frac{\partial^2 M}{\partial r^2}\right]\right\} \tag{8}$$

$$\sigma_{\theta\theta} = 2G\left\{\frac{1}{r}\frac{\partial \phi}{\partial r} - K\tau + \frac{\partial}{\partial z}\left[\nu\nabla^2 M - \frac{1}{r}\frac{\partial M}{\partial r}\right]\right\} \tag{9}$$

$$\sigma_{zz} = 2G\left\{\frac{\partial^2 \phi}{\partial z^2} - K\tau + \frac{\partial}{\partial z}\left[(2-\nu)\nabla^2 M - \frac{\partial^2 M}{\partial z^2}\right]\right\} \tag{10}$$

and

$$\sigma_{rz} = 2G\left\{\frac{\partial^2 \phi}{\partial r \partial z} + \frac{\partial}{\partial r}\left[(1-\nu)\nabla^2 M - \frac{\partial^2 M}{\partial z^2}\right]\right\} \tag{11}$$

where G and v are the shear modulus and Poisson's ratio respectively.
For traction free surface stress functions

$$\sigma_{rr} = \sigma_{rz} = 0 \; at \;\; r = a, \; -h \le z \le h \tag{12}$$

Equations (1) to (12) constitute mathematical formulation of the problem.

Solution

Temperature change

To obtain the expression for temperature T (r, z), we introduce the finite Hankel transform over the variable r and its inverse transform defined by [5] as

$$\bar{T}(\beta_m, z) = \int_0^a r\, K_0(\beta_m, r)\; T(r,z)\; dr \tag{13}$$

$$T(r,z) = \sum_{m=1}^{\infty} K_0(\beta_m, r)\; \bar{T}(\beta_m, z) \tag{14}$$

$$where\; K_0(\beta_m, r) = \frac{\sqrt{2}}{a}\, \frac{J_0(\beta_m r)}{J_0(\beta_m a)}, \tag{15}$$

$\beta_1, \beta_2 \ldots..$ are roots of transcendental equation

$$J_0{}'(\beta_m a) = 0 \tag{16}$$

where $J_n(x)$ is Bessel function of the first kind of order n.

On applying the finite Hankel transform defined in the Eq. (13) and its inverse transform defined in Eq. (14) to the Eq. (2), one obtains the expression for temperature as

$$T(r,z) = \sum_{m=1}^{\infty} \frac{\sqrt{2}}{a} \frac{J_0(\beta_m r)}{J_0(\beta_m a)} \left\{ \begin{matrix} A(\beta_m, -h)\, \frac{\sin h[\beta_m(z-\xi)]}{\sin h[(\beta_m+\xi)\mathrm{h}]} \\ -[A(\beta_m, \xi) - F(\beta_m)]\, \frac{\sin h[\beta_m(z+h)]}{\sin h[(\beta_m+\xi)\mathrm{h}]} + A(\beta_m, z) \end{matrix} \right\} \tag{17}$$

where F (β_m) is the Hankel transform of f(r) and A(β_m,z) is particular integral of differential Eq.(2).

Michells function M

Now we select M which satisfy Eq. (7) is given by

$$M = K \sum_{m=1}^{\infty} F(\beta_m)\; \frac{\sqrt{2}}{a}\; \frac{J_0(\beta_m r)}{J_0(\beta_m a)} \left\{ \begin{matrix} B_m \sinh[\beta_m(z+\mathrm{h})] \\ + C_m\, \beta_m(z+\mathrm{h}) \cosh[\beta_m(z+\mathrm{h})] \end{matrix} \right\} \tag{18}$$

where B_m *and* C_m are arbitrary functions.

Goodiers Thermoelastic Displacement Potential ϕ(r,z)

Assuming the displacement function ϕ(r,z) which satisfies Eq. (1) as

$$\phi(r,z) = \mathrm{K} \sum_{\mathrm{m}=1}^{\infty} \frac{\sqrt{2}}{a}\; \frac{J_0(\beta_m r)}{J_0(\beta_m a)} \times \left\{ \begin{matrix} A(\beta_m, -h)\, \frac{\sin h[\beta_m(z-\xi)]}{\sin h[(\beta_m+\xi)\mathrm{h}]} \\ -[A(\beta_m, \xi) - F(\beta_m)]\, \frac{\sin h[\beta_m(z+h)]}{\sin h[(\beta_m+\xi)\mathrm{h}]} + A(\beta_m, -h)\; e^{\beta_m(\mathrm{z+h})} \end{matrix} \right\} \tag{19}$$

Now using Eqs. (17), (18) and (19) in Eqs. (8), (9), (10) & (11), one obtains the expressions for stresses respectively as

$$\frac{\sigma_{rr}}{K} = 2G\sum_{m=1}^{\infty} \frac{\sqrt{2}}{a\,J_0(\beta_m a)} \quad -\left[\beta_m{}^2 J_1{}'(\beta_m r) + J_0(\beta_m r)\right]$$

$$\times \left[A(\beta_m,-h)\frac{\sin h[\beta_m(z-\xi)]}{\sin h[(\beta_m+\xi)\mathrm{h}]} + [F(\beta_m) - A(\beta_m,\xi)]\frac{\sin h[\beta_m(z+h)]}{\sin h[(\beta_m+\xi)\mathrm{h}]}\right]$$

$$-\left[\beta_m{}^2 J_1'(\beta_m r)\,A(\beta_m,-h)e^{\beta_m(z+\mathrm{h})} + J_0(\beta_m r)\,A(\beta_m,z)\right]$$

$$+\beta_m{}^2 F(\beta_m)C_m\begin{bmatrix}\beta_m{}^2 J_1'(\beta_m r)(z+\mathrm{h})\sinh[\beta_m(z+\mathrm{h})\\ [2v\,J_0(\beta_m r) + J_1{}'(\beta_m r)]\beta_m cosh[\beta_m(z+\mathrm{h})]\end{bmatrix}$$

$$+\beta_m{}^3 F(\beta_m)\,B_m\;\; J_1{}'(\beta_m r)\cosh[\beta_m(z+\mathrm{h})] \tag{20}$$

$$\frac{\sigma_{\theta\theta}}{K} = 2G\sum_{m=1}^{\infty}\frac{\sqrt{2}}{a\,J_0(\beta_m a)} \quad -\left[\beta_m\frac{J_1(\beta_m r)}{r} + J_0(\beta_m r)\right]$$

$$\times\left[A(\beta_m,-h)\frac{\sin h[\beta_m(z-\xi)]}{\sin h[(\beta_m+\xi)\mathrm{h}]} + [F(\beta_m) - A(\beta_m,\xi)]\frac{\sin h[\beta_m(z+h)]}{\sin h[(\beta_m+\xi)\mathrm{h}]}\right]$$

$$-\quad\left[\beta_m\frac{J_1(\beta_m r)}{r}A(\beta_m,-h)e^{\beta_m(z+\mathrm{h})} + J_0(\beta_m r)A(\beta_m,z)\right]$$

$$+\beta_m{}^2\,F(\beta_m)C_m\begin{bmatrix}\beta_m{}^2\frac{J_1(\beta_m r)}{r}(z+\mathrm{h})\sinh[\beta_m(z+\mathrm{h})\\ [2v\,\beta_m J_0(\beta_m r) + \frac{J_1(\beta_m r)}{r}]\beta_m cosh[\beta_m(z+\mathrm{h})]\end{bmatrix}$$

$$\frac{\sigma_{zz}}{K} = 2G\sum_{m=1}^{\infty}\frac{\sqrt{2}\,J_0(\beta_m r)}{a\,J_0(\beta_m a)}\quad\left(\beta_m{}^2 - 1\right) \tag{21}$$

$$\times\left[A(\beta_m,-h)\frac{\sin h[\beta_m(z-\xi)]}{\sin h[(\beta_m+\xi)\mathrm{h}]} + [F(\beta_m) - A(\beta_m,\xi)]\frac{\sin h[\beta_m(z+h)]}{\sin h[(\beta_m+\xi)\mathrm{h}]}\right]$$

$$+\beta_m{}^3\,F(\beta_m)C_m\langle\,(1-2v)\cosh[\beta_m(z+\mathrm{h})] - \beta_m(z+\mathrm{h})\sinh[\beta_m(z+\mathrm{h})\rangle \tag{22}$$

$$\frac{\sigma_{rz}}{K} = 2G\sum_{m=1}^{\infty}\left(-\beta_m{}^2\right)\frac{\sqrt{2}\,J_1(\beta_m r)}{a\,J_0(\beta_m a)}$$

$$\times\quad\left[A(\beta_m,-h)\frac{\cos h[\beta_m(z-\xi)]}{\sin h[(\beta_m+\xi)\mathrm{h}]} + [F(\beta_m) - A(\beta_m,\xi)]\frac{\cos h[\beta_m(z+h)]}{\sin h[(\beta_m+\xi)\mathrm{h}]}\right]$$

$$+A(\beta_m,-h)e^{\beta_m(z+\mathrm{h})} - \beta_m{}^3 F(\beta_m)\,B_m\sinh[\beta_m(z+\mathrm{h})]$$

$$+\beta_m{}^4\,F(\beta_m)C_m\langle\,(-2v)\sinh[\beta_m(z+\mathrm{h})] - \beta_m(z+\mathrm{h})\cosh[\beta_m(z+\mathrm{h})\,\rangle \tag{23}$$

In order to satisfy condition (12), solving equations (20) and (23) for B_m and C_m one obtain,

$$B_m = 0 \tag{24}$$

and

$$C_m = \frac{1}{R}\left[\beta_m{}^2 J_1{}'(\beta_m a) + J_0(\beta_m a)\right]$$

$$\times\left[A(\beta_m,-h)\frac{\sin h[\beta_m(z-\xi)]}{\sin h[(\beta_m+\xi)\mathrm{h}]}+[F(\beta_m)-A(\beta_m,\xi)]\frac{\sin h[\beta_m(z+h)]}{\sin h[(\beta_m+\xi)\mathrm{h}]}\right]$$

$$[\![+\ \beta_m{}^2 J_1'(\beta_m a)A(\beta_m,-h)e^{2\beta_m \mathrm{h}}+J_0(\beta_m a)A(\beta_m,h) \qquad (25)$$

where $R=\beta_m{}^3F(\beta_m)\begin{bmatrix}2\beta_m\mathrm{h}\ J_1{}'(\beta_m a)\sinh(2\beta_m\mathrm{h})\\ \left(2\mathrm{v}\,J_0(\beta_m a)+J_1{}'(\beta_m a)\right)\cosh(2\beta_m\mathrm{h})\end{bmatrix}$

2. SPECIAL CASE AND NUMERICAL CALCULATIONS

Setting

(1) $\mathrm{f(r)}=r^2$

$a=1m,\ h=0.100000000015\ m$

$$F(\beta_m)=\frac{a\sqrt{2}}{J_0(\beta_m a)}[aJ_1(\beta_m a)-2J_2(\beta_m a)]$$

(2) $q(r,z)=\delta(r-r_0)\delta(z-z_0)$

$$\bar{q}(\beta_m,z)=\int_{r'=0}^{a}r'\,\frac{\sqrt{2}}{a}\,\frac{J_0(\beta_m r)}{J_0(\beta_m a)}\,\delta(r-r_0)\delta(z-z_0)\,dr'$$

$$=\frac{\sqrt{2}}{a}\,\frac{\delta(z-z_0)}{J_0(\beta_m a)}r_0\ J_0(\beta_m r_0)$$

where δ(r) is well known diract delta function of argument r.

$r_0=0.5m,\ z_0=0.05m$

3. MATERIAL PROPERTIES

The numerical calculation has been carried out for aluminum (pure) circular plate with the material properties defined as

Thermal diffusivity α = α = $84.18\times10^{-6}\ \mathrm{m^2s^{-1}}$,

Specific heat $c_\rho=896$ J/kg,

Thermal conductivity $k=204.2$ W/m K,

Shear modulus $G=25.5\ G$ pa,

Poisson ratio $\vartheta=0.281$.

4. ROOTS OF TRANSCENDENTAL EQUATION

The $\beta_1=3.8317,\ \beta_2=7.0156,\ \beta_3=10.1735,\ \beta_4=13.3237,\ \beta_5=16.4706,\beta_6=19.6159$ are the roots of transcendental equation $J_0{}'(\beta_m a)=0$. The numerical calculation and the graph has been carried out with the help of mathematical software Mat lab.

5. DISCUSSION

In this problem, a limiting thick circular plate is considered which is subjected to arbitrary known interior temperature and determined the expressions for temperature, displacement and stresses. Here we compute the effects of internal heat generation in terms of stresses along radial direction by substituting q=0 in Eqs. (17), (19), (20), (21), (22), (23), (24) and (25) and we plotted the graphs for stresses for q=0 and q≠0. As a special case mathematical model is constructed for f(r)= r^2 and performed numerical calculation by considering aluminum (pure) circular plate with the material properties specified above.

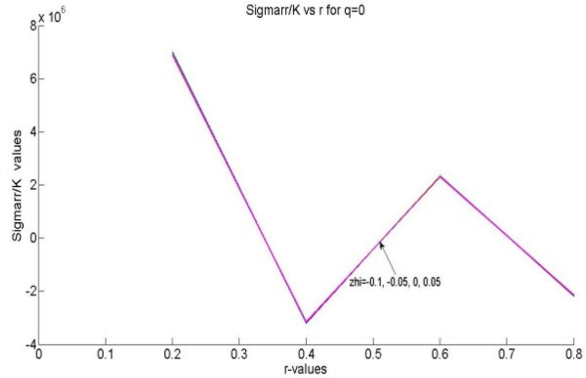

Figure 1 Radial stresses $\frac{\sigma_{rr}}{K}$/ for $q = 0$.

From figure 1, it is observed that the radial stresses $\frac{\sigma_{rr}}{K}$ for $q = 0$ are decreasing for $0.2 \leq r \leq 0.4$, $0.6 \leq r \leq 0.8$ and increasing for $0.4 \leq r \leq 0.6$ along radial direction.

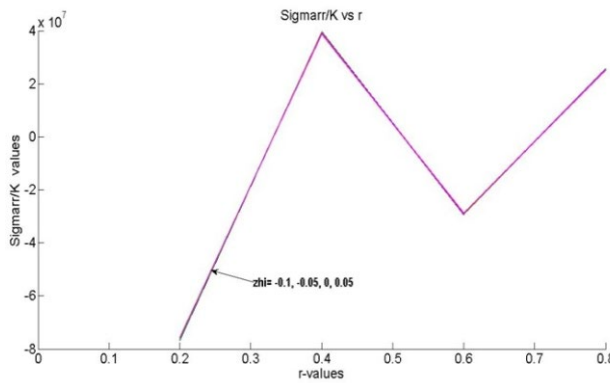

Figure 2 Radial stresses $\frac{\sigma_{rr}}{K}$for $q \neq 0$.

From figure 2, it is observed that the radial stress $\frac{\sigma_{rr}}{K}$ for $q \neq 0$ are increasing for $0.2 \leq r \leq 0.4$, $0.6 \leq r \leq$ and decreasing for $0.4 \leq r \leq 0.6$ along radial direction. From figure 1 and 2 the overall behavior of the radial stresses $\frac{\sigma_{rr}}{K}$ due to internal heat generation is increasing and its nature is compressive along radial direction.

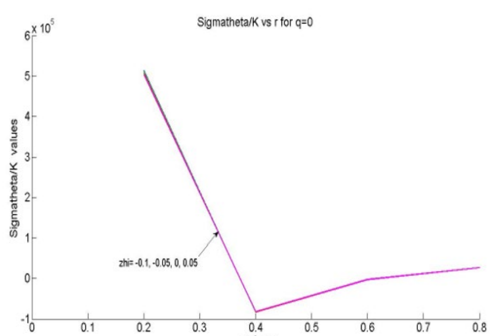

Figure 3 Angular stresses $\frac{\sigma_{\theta\theta}}{K}$ for $q = 0$.

From figure 3, it is observed that the angular stresses $\frac{\sigma_{\theta\theta}}{K}$ for $q = 0$ are decreasing for $0.2 \leq r \leq 0.4$ and increasing for $0.4 \leq r \leq 0.8$ along radial direction.

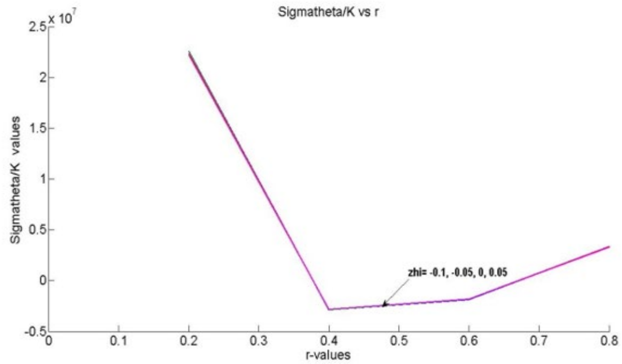

Figure 4 Angular stresses $\frac{\sigma_{\theta\theta}}{K}$for $q \neq 0$.

From figure 4, it is observed that the angular stresses $\frac{\sigma_{\theta\theta}}{K}$ for $q \neq 0$ are decreasing for $0.2 \leq r \leq 0.4$ and increasing for $0.4 \leq r \leq 0.6$ and rapidly for $0.6 \leq r \leq 0.8$ along radial direction.

From figure 3 and 4 due to internal heat generation the overall behavior of the angular stresses $\frac{\sigma_{\theta\theta}}{K}$ are increasing and its nature is compressive along radial direction.

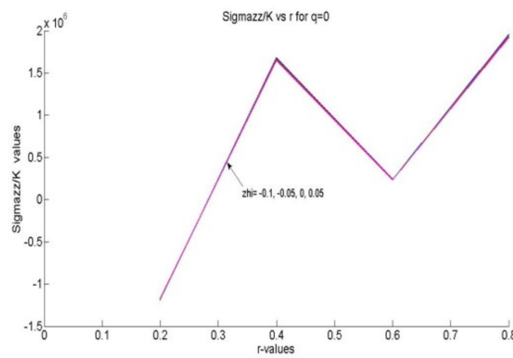

Figure 5 Axial stresses $\frac{\sigma_{zz}}{K}$ for $q = 0$.

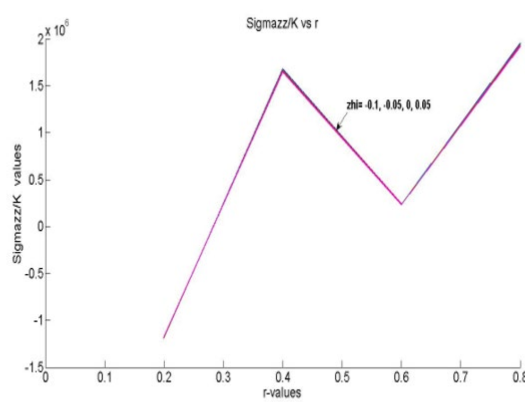

Figure 6 Axial stresses $\frac{\sigma_{zz}}{K}$ for $q \neq 0$.

From figure 5 and 6, it is observed that the axial stresses $\frac{\sigma_{zz}}{K}$ are increasing for $0.2 \le r \le 0.4$, $0.6 \le r \le 0.8$ and decreasing for$0.4 \le r \le 0.6$ along radial direction.

From figure 5 and 6 the overall behavior of the axial stresses $\frac{\sigma_{zz}}{K}$ due to internal heat generation is tensile in nature along radial direction.

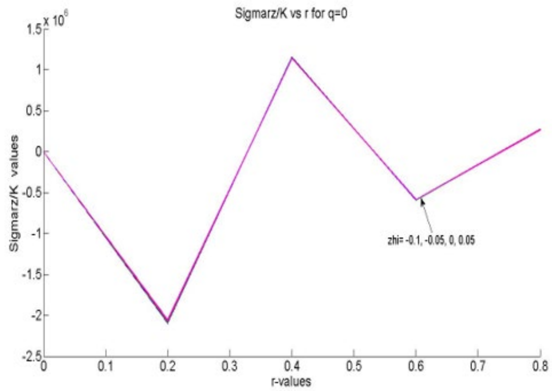

Figure 7 Stresses $\frac{\sigma_{rz}}{K}$ for $q = 0$.

From figure 7, it is observed that the stresses $\frac{\sigma_{rz}}{K}$ for $q = 0$ are decreasing for $0 \le r \le 0.2, 0.4 \le r \le 0.6$ and increasing for $0.2 \le r \le 0.4$, $0.6 \le r \le 0.8$ along radial direction.

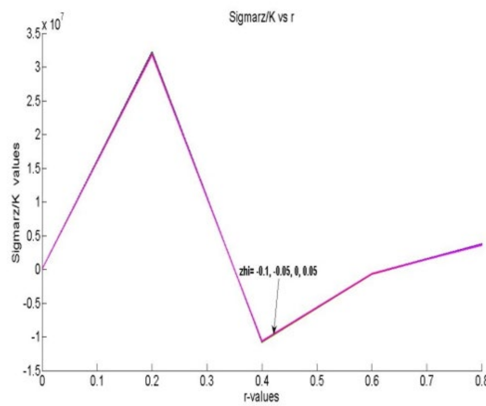

Figure 8 Stresses $\frac{\sigma_{rz}}{K}$ for $q \neq 0$.

From figure 8, it is observed that the stress $\frac{\sigma_{rz}}{K}$ for $q \neq 0$ are increasing for $0 \le r \le 0.2$, $0.4 \le r \le 0.8$ and decreasing for $0.2 \le r \le 0.4$ along radial direction.

From figure 7 and 8 the overall behavior of the stress $\frac{\sigma_{rz}}{K}$ due to internal heat generation is increasing and its nature is compressive along radial direction.

6. CONCLUSION

Due to internal heat generation the radial stresses $\frac{\sigma_{rr}}{K}$, the axial stresses$\frac{\sigma_{zz}}{K}$, the stresses$\frac{\sigma_{rz}}{K}$ and the angular stresses$\frac{\sigma_{\theta\theta}}{K}$ are increased along radial direction. The radial stresses, the angular stresses and the stresses $\frac{\sigma_{rz}}{K}$ are compressive in nature whereas the axial stresses $\frac{\sigma_{zz}}{K}$are tensile in nature along radial direction.

The results obtained here are useful in engineering problems particularly in the determination of state of stress in a thick circular plate, base of furnace of boiler of a thermal power plant, gas power plant and the measurement of aerodynamic heating.

CONFLICT OF INTERESTS

None.

ACKNOWLEDGMENTS

None.

REFERENCES

Bhongade C. M. and Durge M. H. (2013) Effect of Michell function on steady state behavior of thick circular Plate. IOSR Journal of Mathematics 8, 55-60.

Kulkarni V. S. and Deshmukh K. C. (2008) An inverse quasi- static steady state thermal stresses in a thick circular plate in a thick circular plate. The Journal of Franklin Institute 345, 29-38.

Naotake Noda, Richard B Hetnarski and Yoshinobu Tanigawa (2003) Thermal Stresses, 2 nd edn., Taylor and Francis, New York, 259-261.

Noda N., Ashida F. and Tsuji T. (1989) An inverse transient thermoelastic problem of a transversely isotropic solid. Journal of applied Mechanics (Trans. of the Asme, Ser. E) 56, 791-797.

M. N. Ozisik (1968) Boundary Value Problems of Heat Conduction, International Text Book Company, Scranton, Pennsylvania.